Introduction of Geothermal Power Plant

.....

Dr.-Ing. Ir. Nasruddin, M.Eng

Course: Operators of Geothermal Powerplants

UI, Jakarta, 5,6 & 7 August 2017

Hosting by: GEOCAP, PPSDM EBTKE, Jakarta

GPP SYSTEM

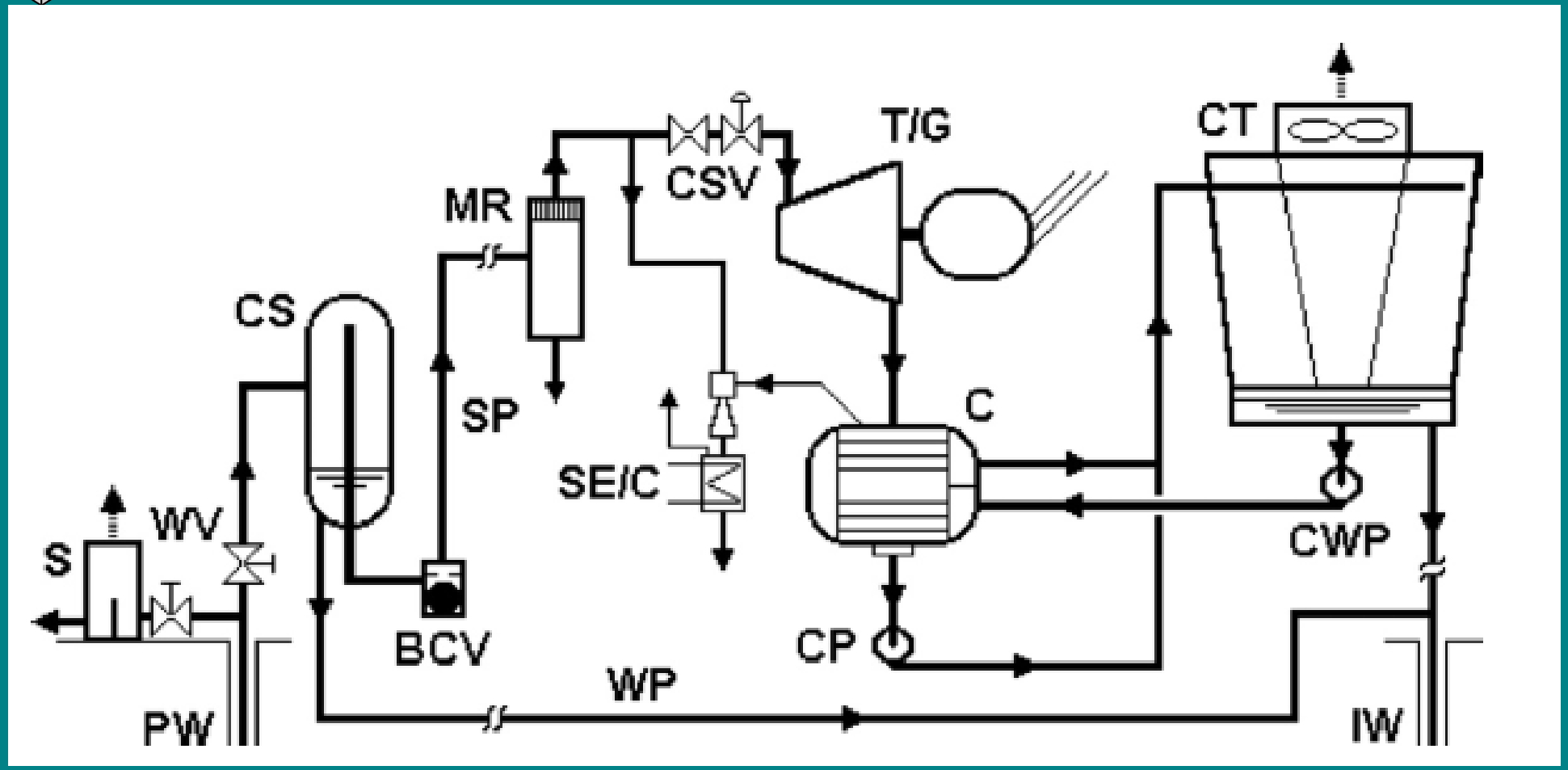

DiPippo, Ronald, Geothermal power plants : principles, applications, case studies, and environmental impact. 3rd ed, 2012

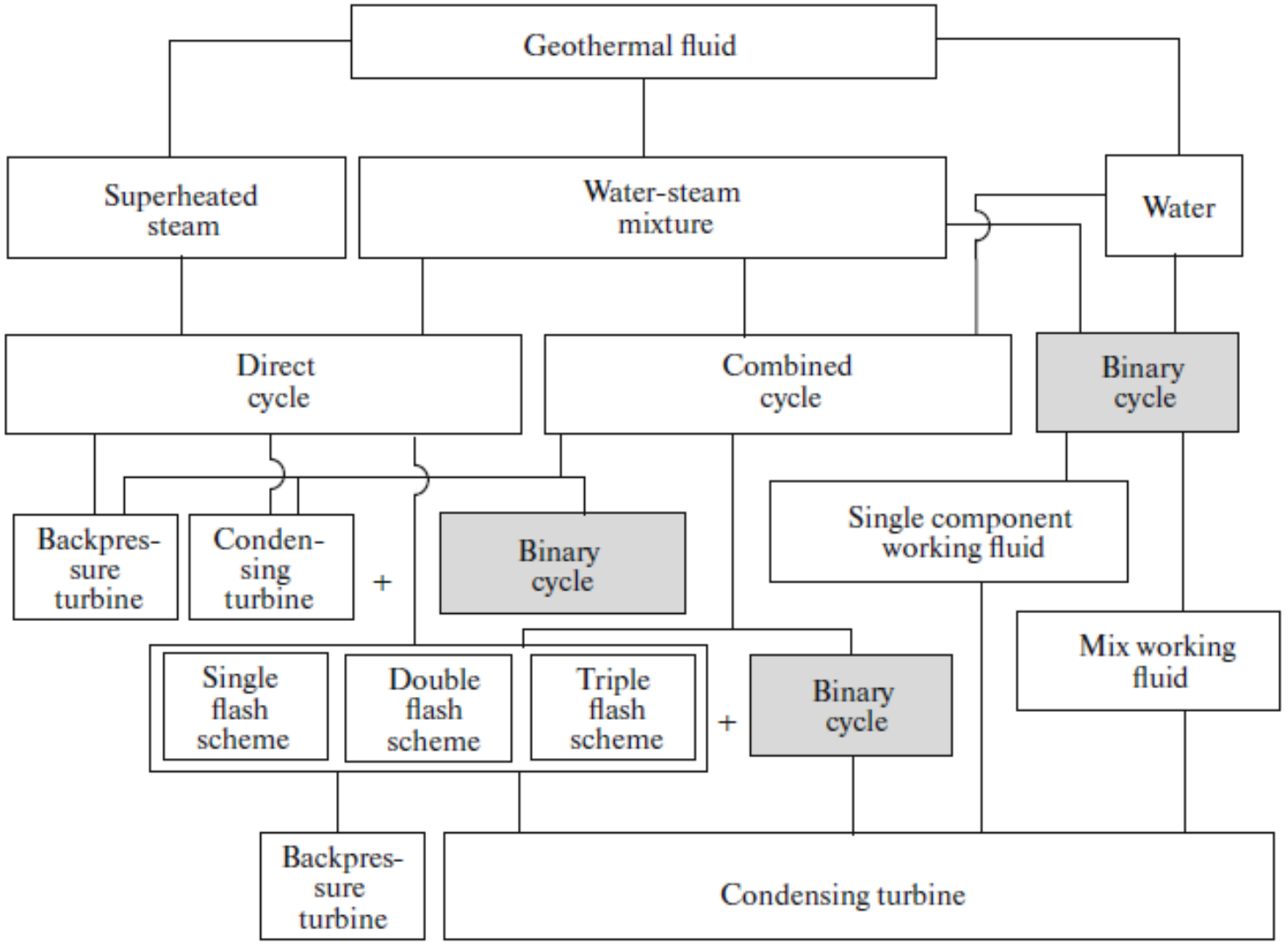

Fig. 1. Classification of GeoPPs by a phase state and applied process flow diagrams.

G. V. Tomarov and A. A. Shipkov, Modern Geothermal Power: GeoPP with Geothermal Steam Turbines, *Thermal Engineering, 2017, Vol. 64, No. 3, pp. 190–200.*

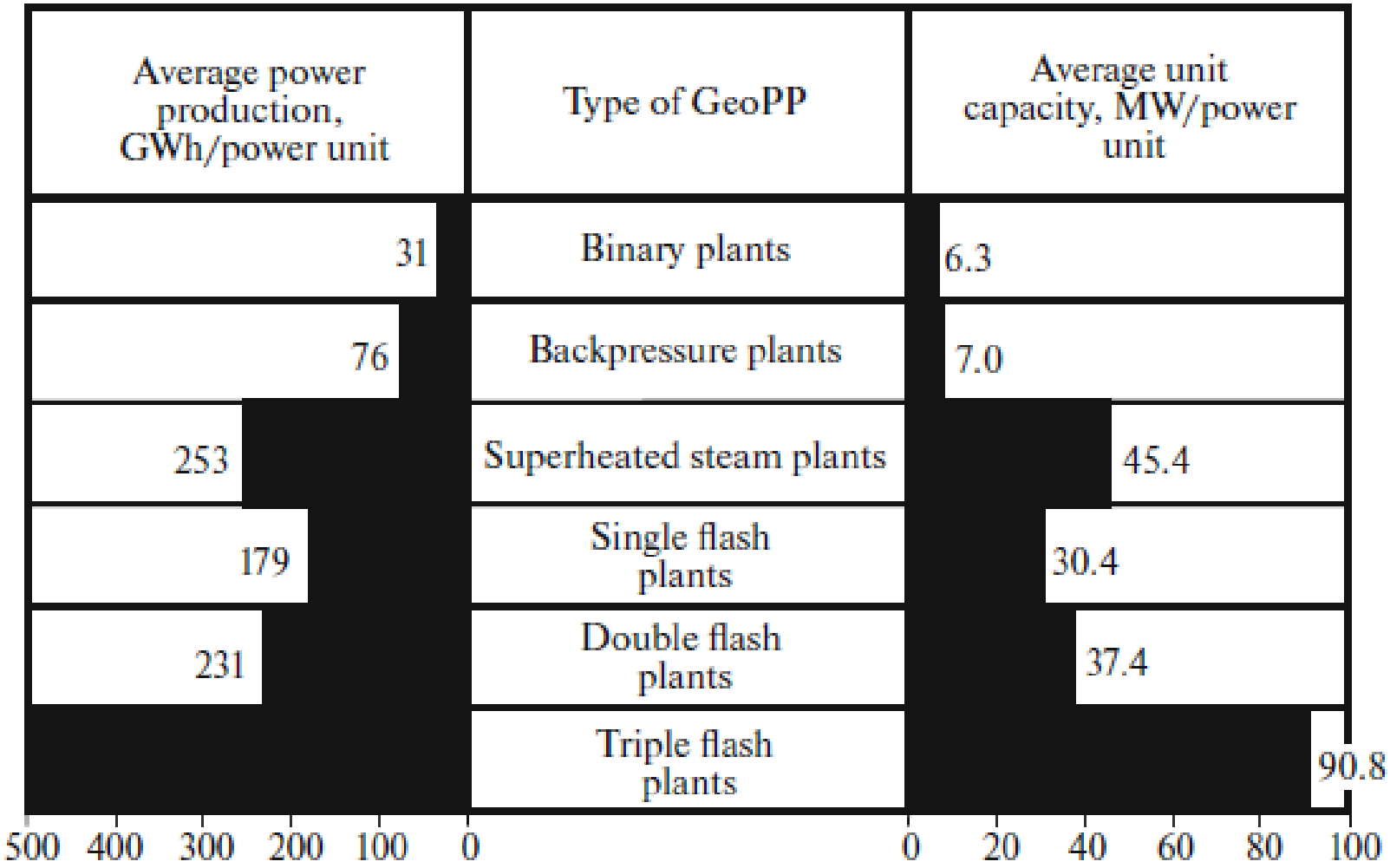

Fig. 4. Average unit capacity and power generation per one power unit for various types of GeoPPs.

G. V. Tomarov and A. A. Shipkov, Modern Geothermal Power: GeoPP with Geothermal Steam Turbines, *Thermal Engineering, 2017, Vol. 64, No. 3, pp. 190–200.*

Steam Cycle System

Single Flash Steam Cycle

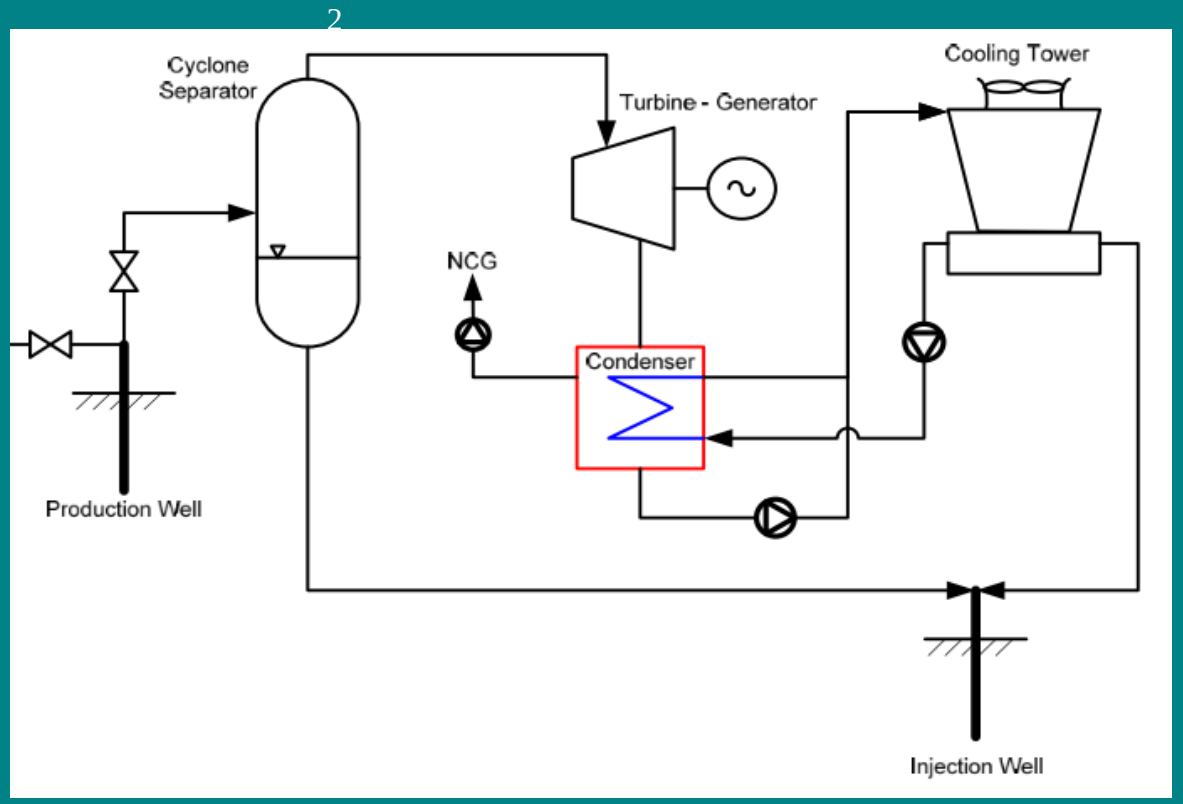

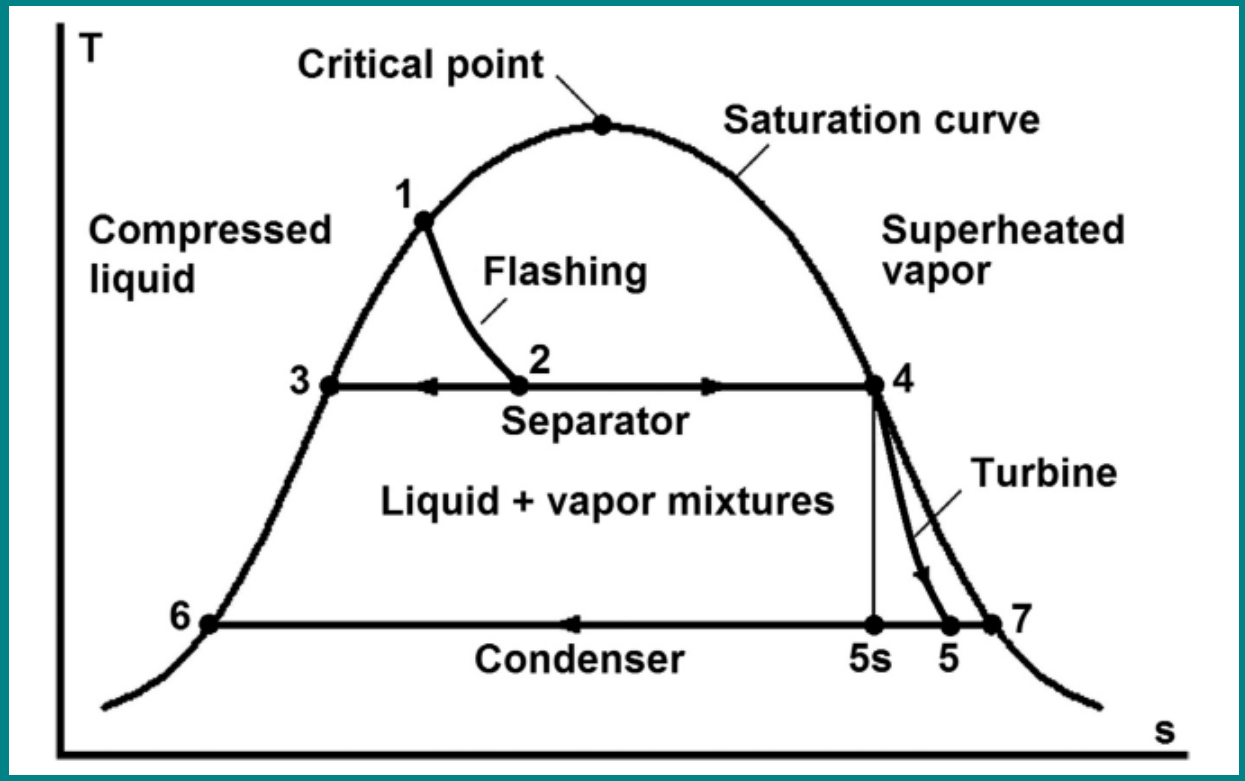

DiPippo, Ronald, Geothermal power plants : principles, applications, case studies, and environmental impact. 3rd ed, 2012

Steam Cycle System

Double Flash Steam Cycle

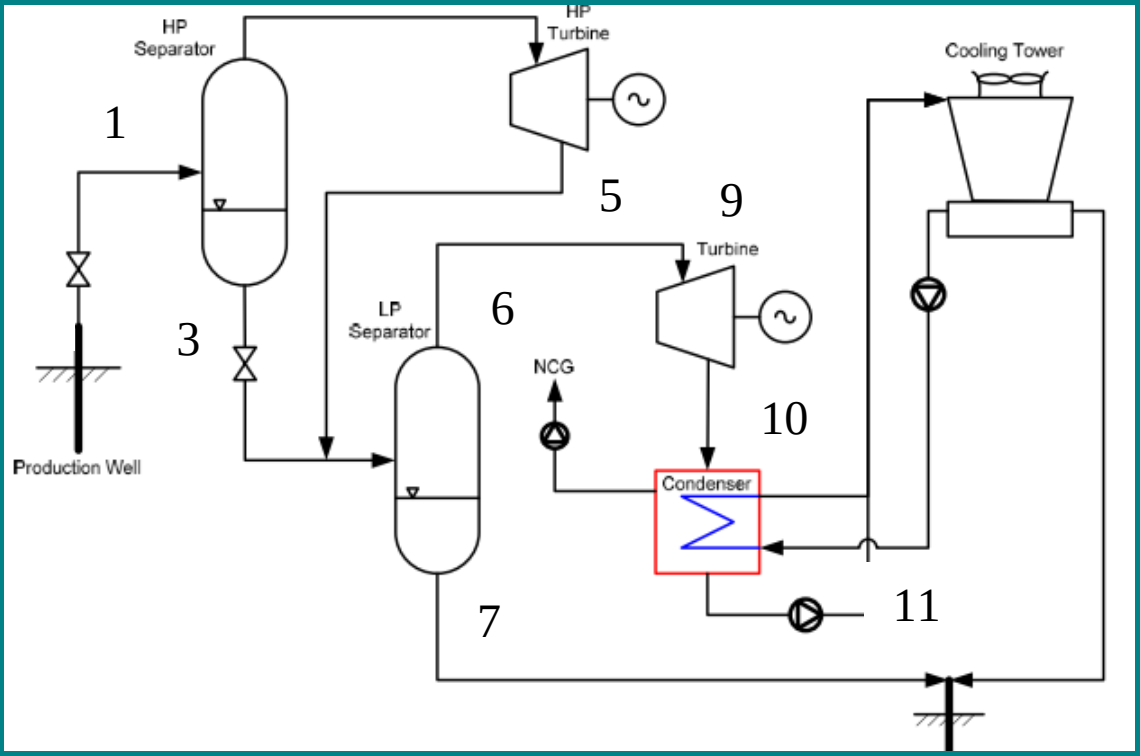

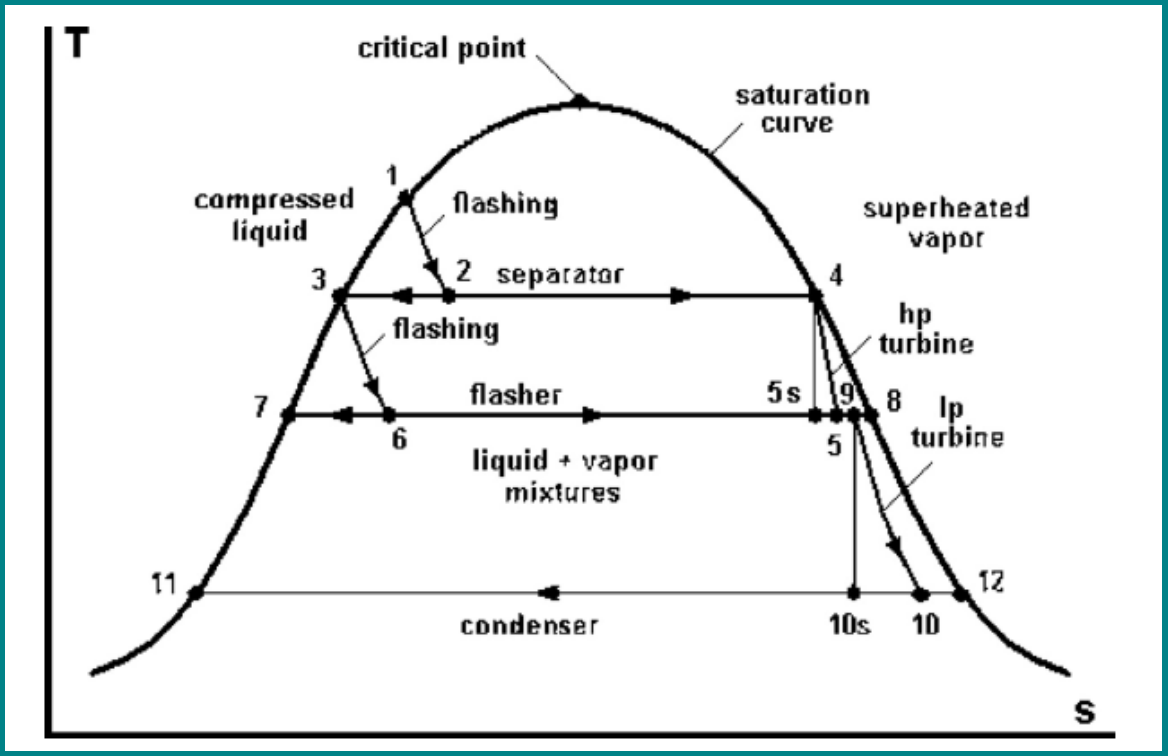

DiPippo, Ronald, Geothermal power plants : principles, applications, case studies, and environmental impact. 3rd ed, 2012

SEPARATOR

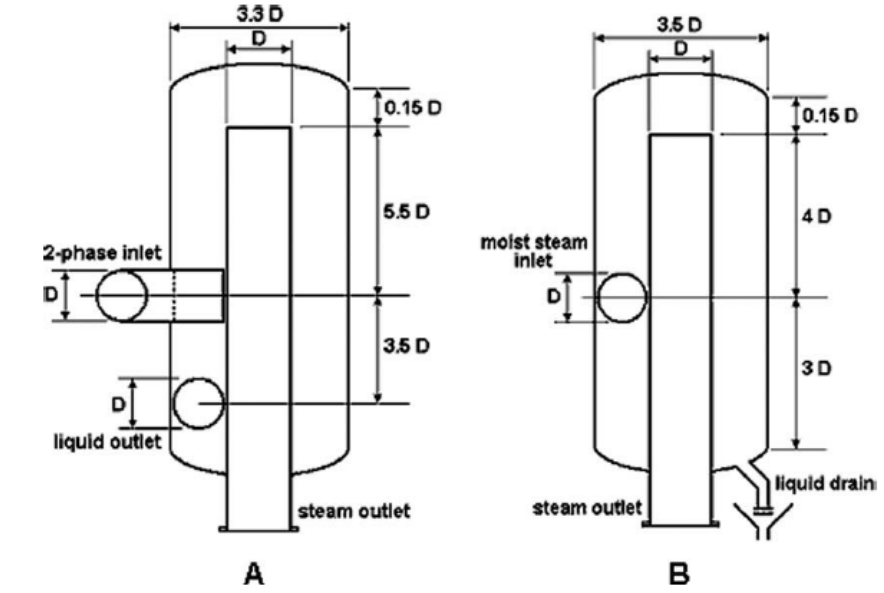

Fig. 5.8 General design specifications for cyclone separator (A) and cyclone moisture remover (B) [7].

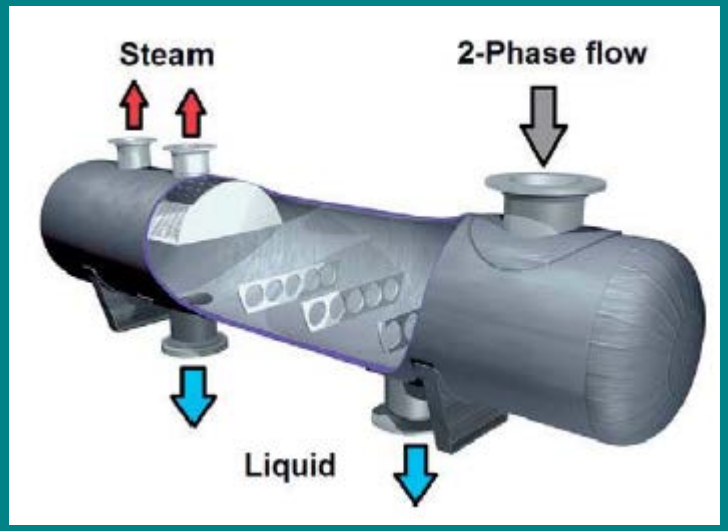

Table 5.1 Separator and moisture remover design guidelines [7].

Parameter	Separator	Moisture remover
Maximum steam velocity at the 2-phase inlet pipe	45 m/s (150 ft/s)	60 m/s (195 ft/s)
Recommended range of steam velocity at the 2-phase inlet pipe	25–40 m/s (80–130 ft/s)	35–50 m/s (115–160 ft/s)
Maximum upward annular steam velocity inside cyclone	4.5 m/s (14.5 ft/s)	6.0 m/s (20 ft/s)
Recommended range of upward annular steam velocity inside cyclone	2.5–4.0 m/s (8–13 ft/s)	1.2–4.0 m/s (4–13 ft/s)

Ronald DiPippo (Auth.)-Geothermal Power Plants. Principles, Applications, Case Studies and Environmental Impact-Butterworth-Heinemann (2013)

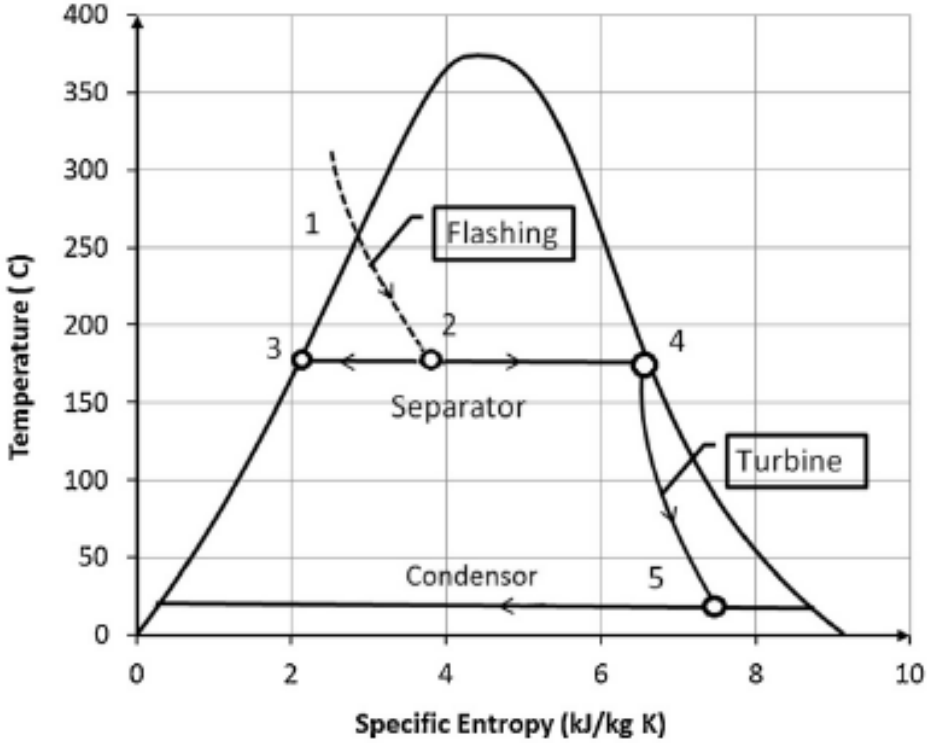

Fig. 4. Temperature entropy diagram for typical single flash plant.

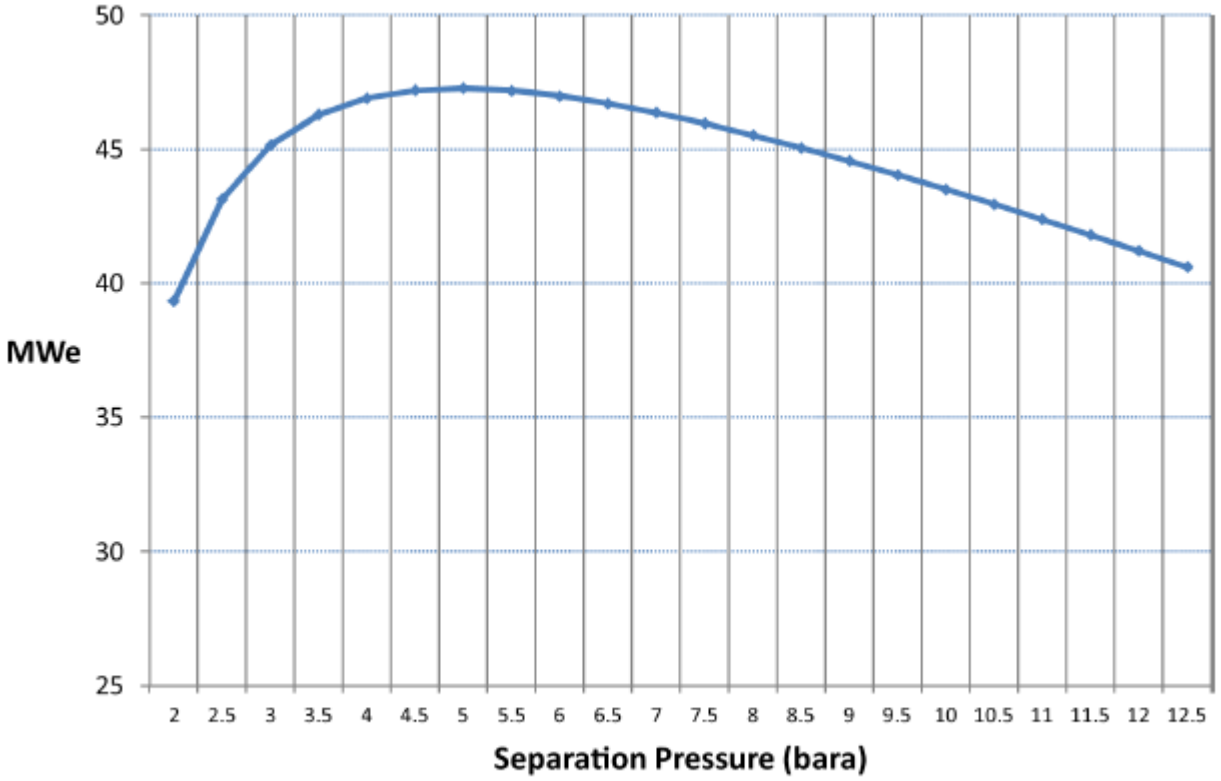

Fig. 5. Generated power vs separation pressure.

S.J. Zarrouk, M.H. Purnanto / Geothermics 53 (2015) 236–254

Table 1
Geothermal separators used around the world.

Country	Field	Unit	Year	Type	MW rated	Sep. type	Notes	Ref.
Costa Rica	Miravalle	Wellhead Unit 1	1995	1-Flash backpressure	1 × 5	V.	Wellhead unit 1 and wellhead unit 3 have been dismantled in 1998.	Moya and Nietzen (2005) and Di Pippo (2008)
		Wellhead Unit 2	1996	1-Flash	1 × 5	N.A.	There are 7 separation stations that supply the steam needed for Wellhead Unit 1, Unit 1, Unit 2 and Unit 3. Binary plant uses waste brine from Unit 1, 2 and 3	
		Wellhead Unit 3	1997	1-Flash	1 × 5	N.A.		
		1	1994	1-Flash	1 × 55	V.		
		2	1998	1-Flash	1 × 55	V.		
		3	2000	1-Flash	1 × 29	V.		
		5	2004	Binary	2 × 9.5	V.		
El Salvador	Ahuachapan	1	1975–1976	1-Flash	1 × 30	V.	The horizontal separator in Unit 3 is a flasher that is installed to recover low pressure steam from wasted hot water in Unit 1 and 2	Di Pippo (1980), Kozaki (1982) and Monterrosa and Lopez (2010)
		2	1975–1976	1-Flash	1 × 30	V.		
		3	1980	2-Flash	1 × 35	H.		
El Salvador	Berlin	Wellhead	1992	1-Flash	2 × 5	V.	Wellhead units have been retired	Horie (2001), Di Pippo (2008), Argueta (2011) and Fuji (2011)
		1	1999	1-Flash	1 × 28	V.		
		2	1999	1-Flash	1 × 28	V.		
		3	2006	1-Flash	1 × 40	N.A.		
		4	2007	Binary	1 × 9.2	N.A.		
Indonesia	Wayang Windu	1	2000	1-Flash	1 × 110	V.	There are 3 separators for each unit, sized at 40 MW each	Murakami et al. (2000) and Syah et al. (2010)
		2	2009	1-Flash	1 × 117	V.		
Indonesia	Gunung Salak	1	1994	1-Flash	1 × 55	V.	Gunung Salak is also known as Awibengkok	Soeparjadi et al. (1998), Di Pippo (2008) and Adiprana et al. (2010)
		2	1994	1-Flash	1 × 55	V.		
		3	1997	1-Flash	1 × 55	V.		
		4	1997	1-Flash	1 × 55	V.		
		5	1997	1-Flash	1 × 55	V.		
		6	1997	1-Flash	1 × 55	V.		
Mexico	Cerro Prieto I	1 and 2	1973	1-Flash	2 × 37.5	V.	The gathering system consists of cyclone separators at each well, with steam line to power station and brine line to evaporation pond	Di Pippo (2008)
		3 and 4	1979	1-Flash	2 × 37.5	V.		
		5	1981	2-Flash	1 × 30	V.		
	Cerro Prieto II	1 and 2	1984	2-Flash	2 × 110	V.	The gathering system consists of one pair of wellhead separator and flasher from each well	Di Pippo (2008)
	Cerro Prieto III	1 and 2	1985	2-Flash	2 × 110	V.		
	Cerro Prieto IV	1–4	2000	1-Flash	4 × 25	V.		Di Pippo (2008)
New Zealand	Mokai	1	1999	Flash-Binary	1 × 25, 6 × 5	V.	The hot brine from the separator is passed to the evaporator section of the hot water binary plant. The dry steam is passed into the backpressure steam turbine and delivered to the evaporator section of the binary cycle plant. Mokai 1 has 2 separators while Mokai 2 has only 1 separator	Di Pippo (2008)
		2	2005	Flash-Binary	1 × 34, 1 × 8	V.		
New Zealand	Rotokawa	Combined Cycle	1997	Flash-Binary	1 × 13, 3 × 4.5	V.	The dry steam from the separator is sent to the backpressure turbine. The hot brine from the separator is used for the binary plant. The exhaust steam from the turbine is also used for the binary plant	Legmann (1999), Legmann and Sullivan (2003) and Di Pippo (2008)
		Extension	2003	Binary	1 × 4.5	N.A.		Di Pippo (2008)
		Nga Awa Purua	2010	3-Flash	1 × 139	V.	Inlet steam pressure: HP = 23.5 bara; IP = 8.4 bara; LP = 2.3 bara	Horie (2009)
New Zealand	Kawerau	1	2008	2-Flash	1 × 95	V.	Inlet steam pressure: HP = 11.3 bara; LP = 1.8 bara	Horie (2009)

Table 1 (*Continued*)

Country	Field	Unit	Year	Type	MW rated	Sep. type	Notes	Ref.
New Zealand	Wairakei	The A station, the B station, binary plant	1958–1963	1 Flash, 3-Flash, Binary	Total= 193	V.	The A station consist of several small units rated at 6.5 MW and 11.5 MW. There are HP turbines (12.4 bar), IP turbines (3.45 bar) and LP turbines (0.345 bar). The B station consists of three units, each rated at 30 MW. The turbine was design to take IP steam from the A station	Thain and Carey (2009)
New Zealand	Ohaaki	1	1989	1-Flash	1 × 104	V.	Operating capacity is 70 MW	From author's experience
New Zealand	Te Huka	1	2010	Binary	1 × 23	V.	Also known as Tauhara 1	From author's experience
Iceland	Nesjavellir	1 and 2	1998	1-Flash	2 × 30	H.	The separation system consists of steam separators and mist eliminators. The brine and exhaust steam from the turbine are both used to heat the water for domestic use in Reykjavic	Eliasson (2001) and Di Pippo (2012)
		3	2001	1-Flash	1 × 30	H.		
		4	2005	1-Flash	1 × 30	H.		
Iceland	Hellisheidi	1 and 2	2006	1-Flash	2 × 45	H.	It was initially designed as an electric generating station and then later became a cogeneration heat and power plant. Unit 3 is low pressure turbine, taking advantage of large volume of hot water from Units 1 and 2 separator. There are three separations stations with 21 water-steam separators in total	Di Pippo (2012) and Gunnlaugsson (2012)
		3	2007	1-Flash	1 × 33	H.		
		4 and 5	2008	1-Flash	2 × 45	H.		
		6 and 7	2011	1-Flash	2 × 45	H.		
Iceland	Krafla	1	1978	2-Flash	1 × 30	V.	Initially, wellhead separators were installed for each well pad. They were replaced with a centralised separation station. Due to ineffectiveness	Juliusson et al. (2005)
Iceland	Svartsengi	PP-1	1977	1-Flash	2 × 1	N.A.	The turbines are the backpressure type	Thorolfsson (2005), Albertsson et al. (2010) and Di Pippo (2012)
		PP-2	1981	–	–	–	PP-2 is not used for electricity generation. It is used for district heating with capacity 3 × 25 MWth	
		PP-3	1981	1-Flash	1 × 6	V.	The turbine is the backpressure type. The separator is located close to the turbine	
		PP-4	1989, 1993	Binary	3 × 1.2, 4 × 1.2	N.A.	It was the first time in the world an Ormat's ORC unit was directly connected to a backpressure turbine as a bottoming unit	
		PP-5	1999	1-Flash	1 × 30	H.	The steam supply system comprises a horizontal separator and a horizontal moisture separator, both with mist eliminator pads	
		PP-6	2007	Dry Steam	1 × 30	–	–	
Russia	Mutnovsky	1	2002	1-Flash	2 × 25	H.	All equipment except the two-phase pipeline is located inside the building to protect the plant equipment and personnel from the harsh winter weather. One building is used as the power house, while another building is used as a separator building	Povarov et al. (2003) and Di Pippo (2012)
Russia	Verkhne-Mutnovsky	1	1998	1-Flash	1 × 4	H.	The separated brine is flashed to be used by steam jet ejectors for non-condensable gas removal. The unique feature of this plant is the use of an air-cooled condenser normally found in a binary plant	Di Pippo (2012)
		2 and 3	1999	1-Flash	2 × 4	H.		
United States of America	Beowawe	1	1985	2-Flash	1 × 16	V., H.	The vertical separator is used to separate steam and water while the horizontal separator is used as a flasher for the hot brine produced from the vertical one	Di Pippo (2008) and Di Pippo (2012)

S.J. Zarrouk, M.H. Purnanto / Geothermics 53 (2015) 236–254

S.J. Zarrouk, M.H. Purnanto / Geothermics 53 (2015) 236–254

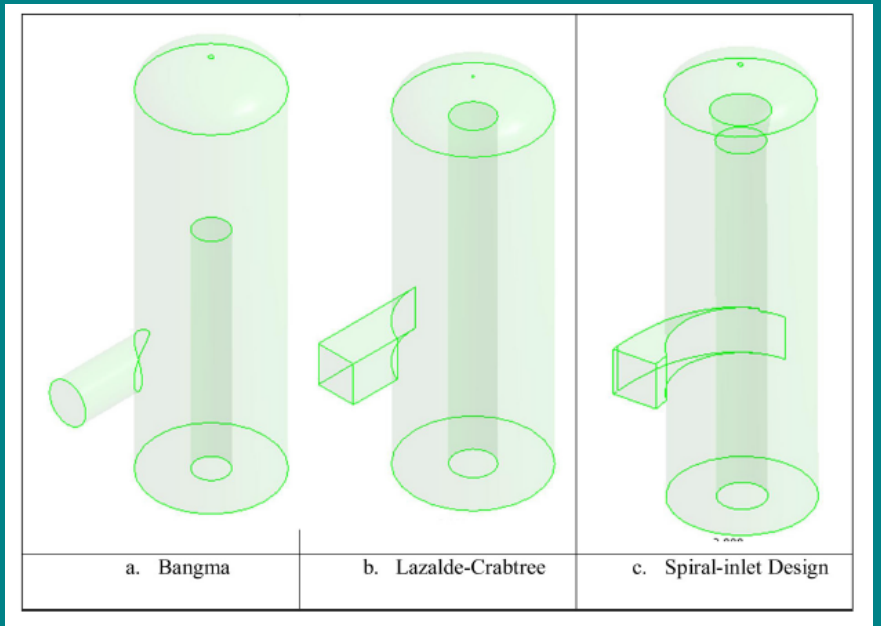

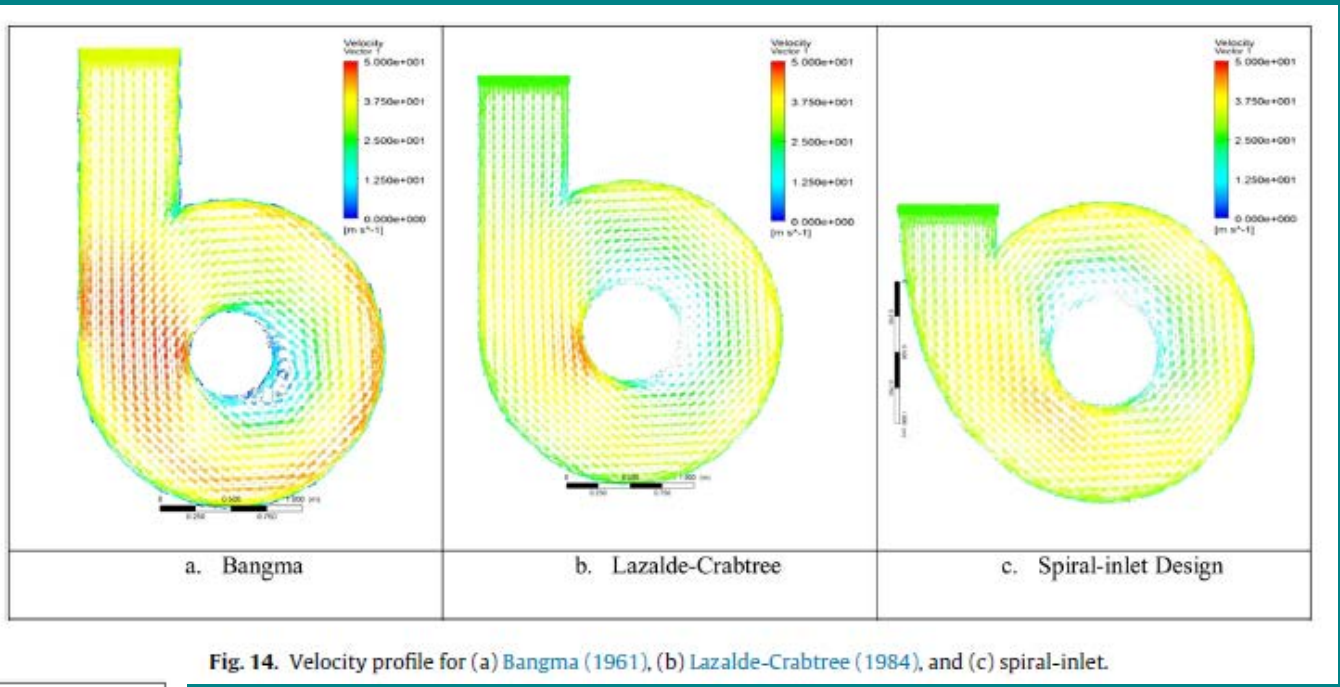

Fig. 14. Velocity profile for (a) Bangma (1961), (b) Lazalde-Crabtree (1984), and (c) spiral-inlet.

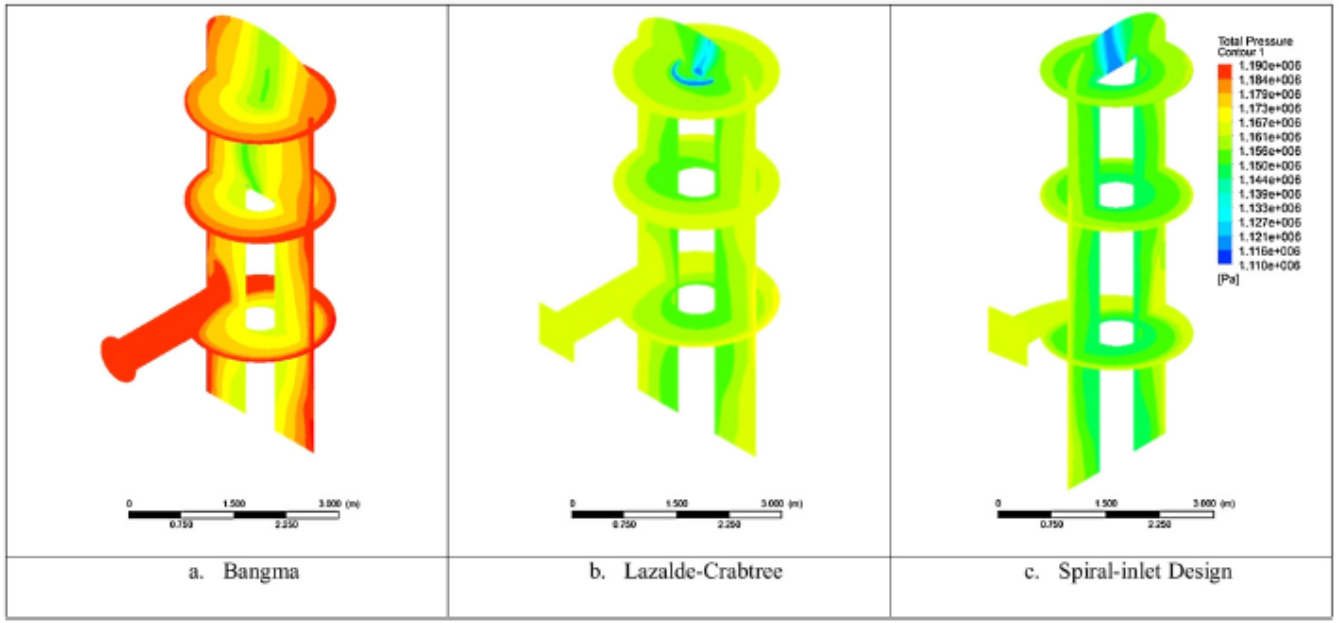

Fig. 16. Standard size distribution for droplets in pipelines (after Hoffmann and Stein, 2007).

S.J. Zarrouk, M.H. Purnanto / Geothermics 53 (2015) 236–254

TURBINE

Table 5.2 Typical turbine element materials [10].

Component	Material
Piping	ASTM A106, Gr B; ASTM A335, Gr P11 or P22
H.P. casings	ASTM A356, Gr 1, 6, 9, or 10
L.P. casings	ASTM A285 or A515
Valve bodies	ASTM A216 or A217
Fasteners	ASTM A193 and A194
Rotors	ASTM A470
Blades	AISI 403
Nozzle blades	AISI 403
Bands	AISI 405

DiPippo, Ronald-Geothermal Power Plants - Principles, Applications, Case Studies and Environmental Impact-Elsevier (2012)

Table 2. Main producers of geothermal steam turbines

Company (country)	Main specialization	Total installed capacity of the manufactured turbines, MW
Toshiba (Japan)	Steam turbines and other power equipment	Over 3000
Mitsubishi (Japan)	Geothermal steam turbines and generators	Over 2800 (100 power units)
Fuji (Japan)	Geothermal steam turbines	2630 (67 power units)
General Electric (United States)	As above	Over 500
Toyota (Japan)	As above	Over 250
Ansaldo (Italy)	Major manufacturer of geothermal steam turbines and power equipment	1700 (130 power units)
Alstom (Italy)	50 years of experience in the manufacturing of geothermal steam turbines with a unit capacity of 25–60 MW	200
Kaluga Turbine Works (Russia)	Manufacturer of geothermal turbines with a capacity of 0.5–25 MW	Over 80

G. V. Tomarov and A. A. Shipkov, Modern Geothermal Power: GeoPP with Geothermal Steam Turbines,
Thermal Engineering, 2017, Vol. 64, No. 3, pp. 190–200.

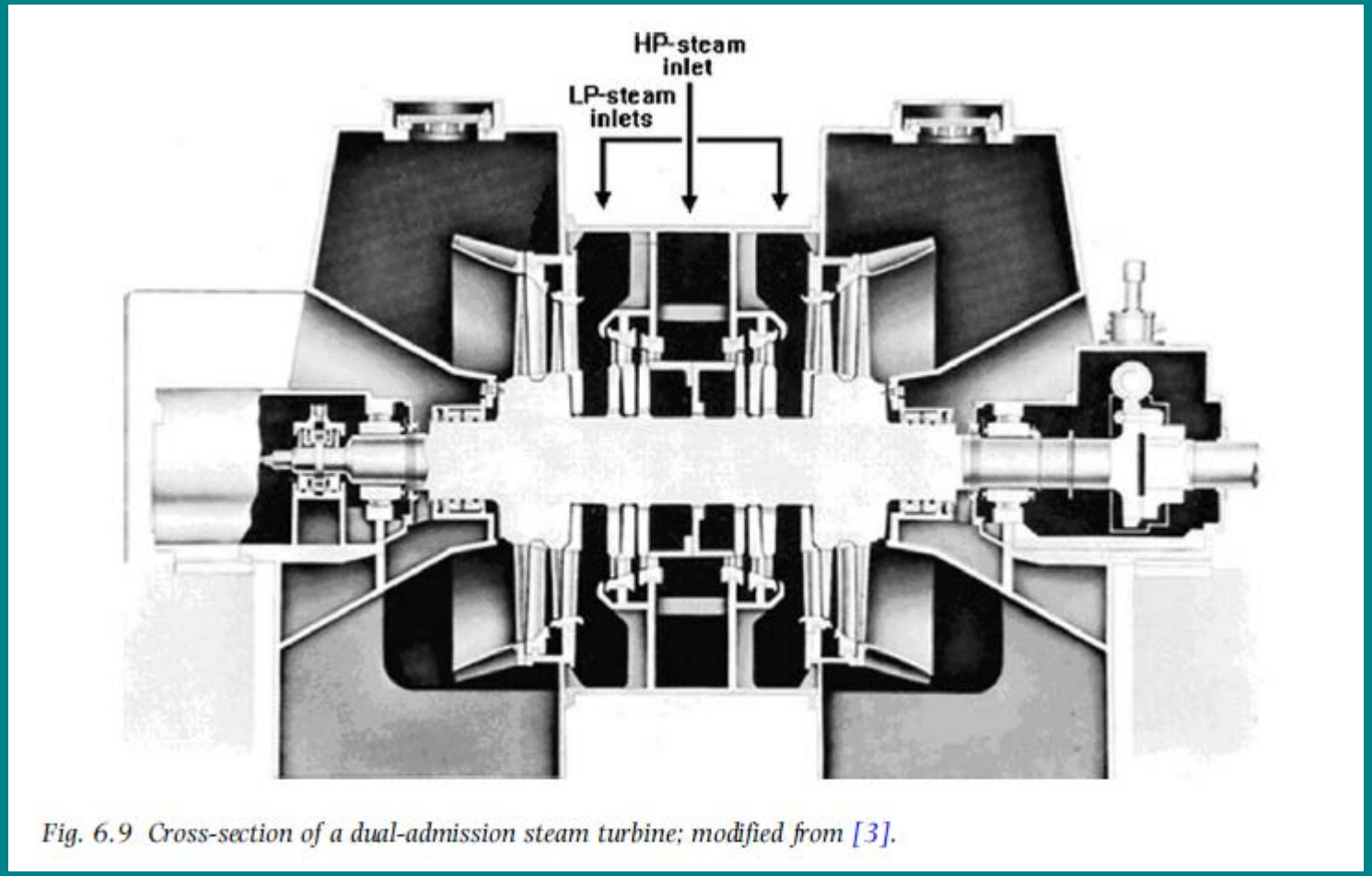

Fig. 6.9 Cross-section of a dual-admission steam turbine; modified from [3].

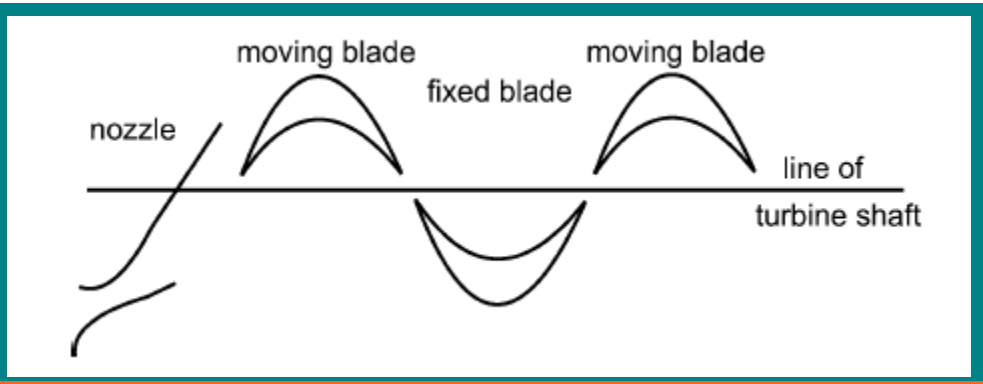

Ronald DiPippo (Auth.)-Geothermal Power Plants. Principles, Applications, Case Studies and Environmental Impact-Butterworth-Heinemann (2013)

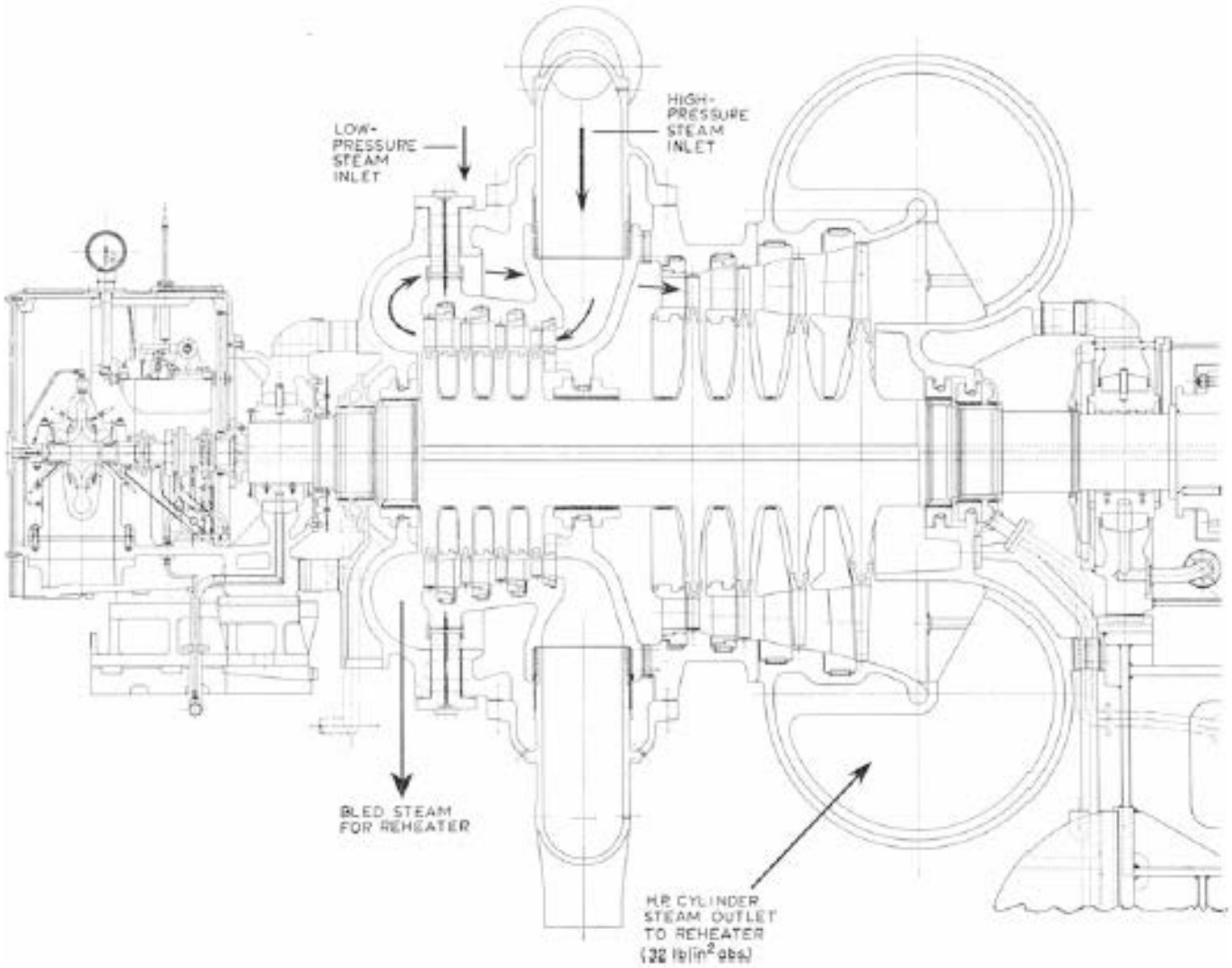

Fig. 11.8 Drawing of part of a 325 MWe mixed pressure turbine illustrating the steam flow path, steam addition after the high-pressure stages and a change in flow direction and passage diameter (reproduced from Worley, Proc (1963–64) by permission of SAGE Publications Ltd.)

Arnold Watson, Geothermal Engineering Fundamentals and Applications, Springer, 2013

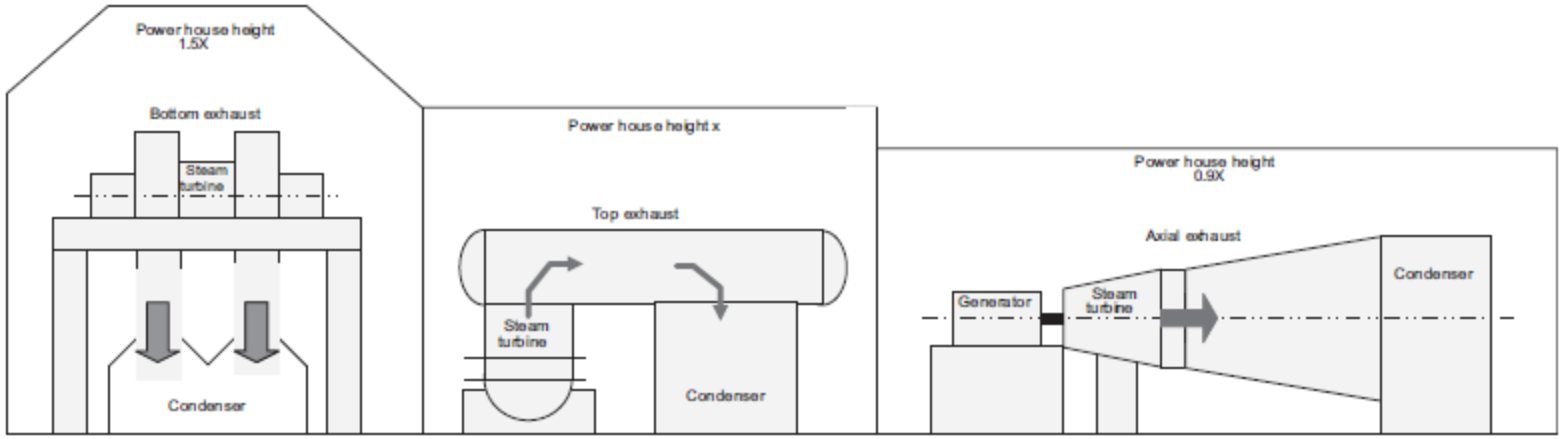

Figure 10.16 Turbine exhaust configurations.
Adapted from MHI. A new geothermal steam turbine with a single cylinder axial exhaust design (outline of the Hellisheidi geothermal turbine in Iceland). Tech Rev December 2007;44(4).

(Woodhead Publishing Series in Energy) Ron DiPippo-Geothermal Power Generation. Developments and Innovation-Woodhead Publishing (2016)

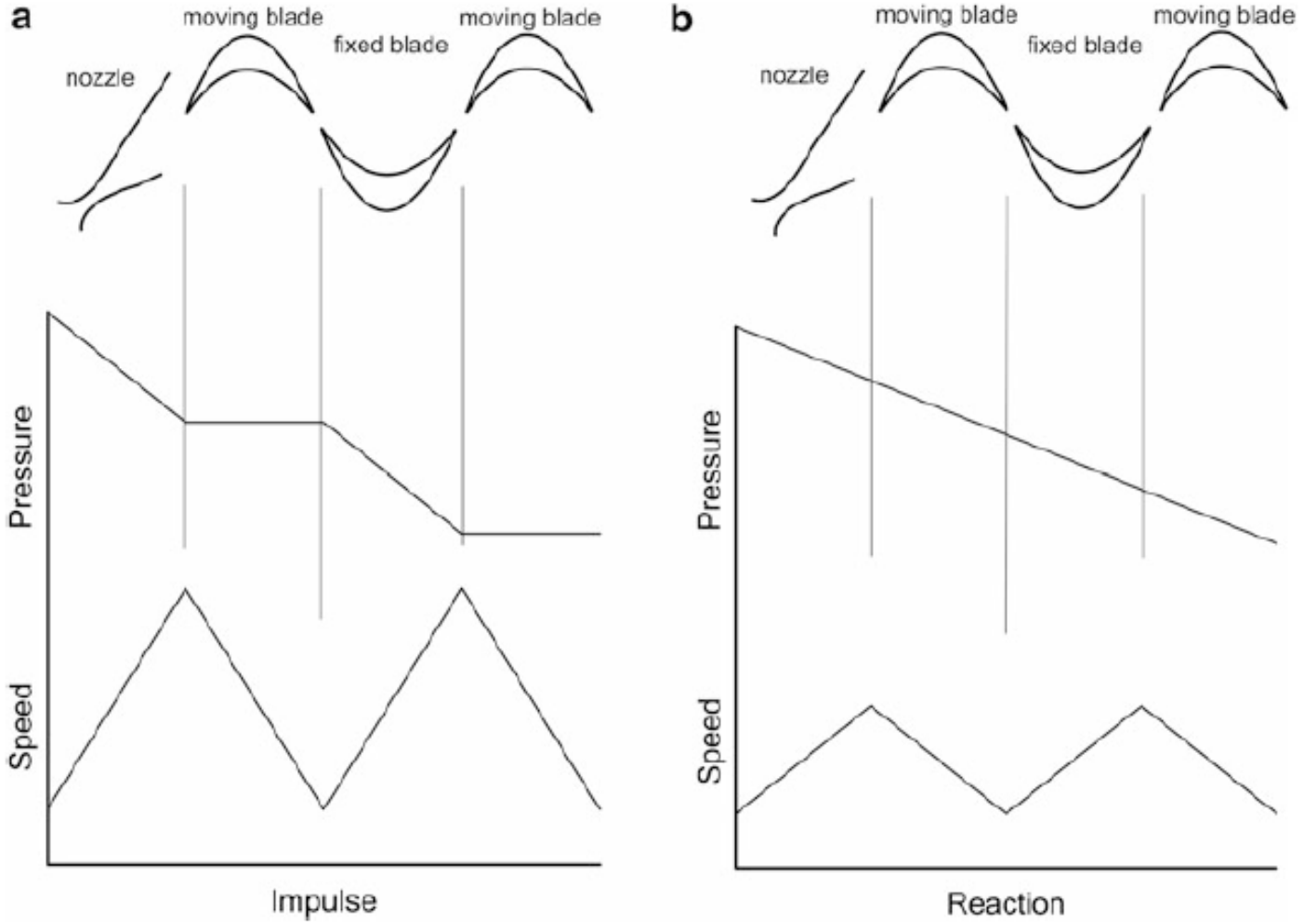

Fig. 11.10 Comparison of the two basic turbine types (a) an impulse turbine and (b) a reaction turbine

Arnold Watson, Geothermal Engineering Fundamentals and Applications, Springer, 2013

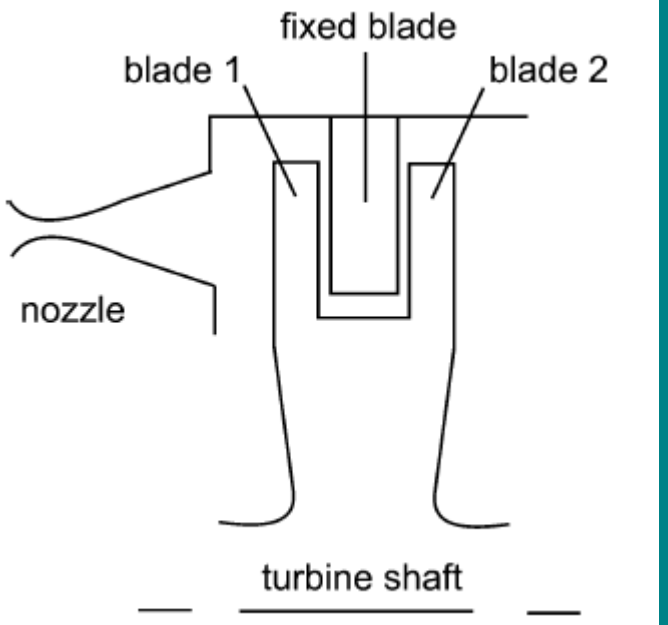

Arnold Watson, Geothermal Engineering Fundamentals and Applications, Springer, 2013

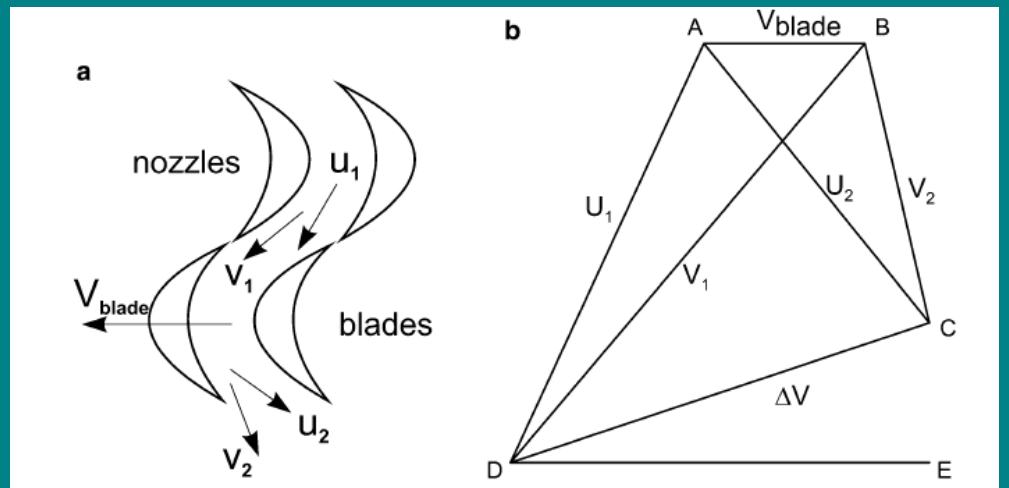

Fig. 11.12 Showing as (a) the flow passages in a nozzle and turbine blade pair and the absolute and relative steam velocities, and (b) the velocity diagram plotted to arrive at the torque and axial thrust of the pair. The axis of rotation (not shown) is vertical

Fig.6 High-load high-efficiency reaction blades

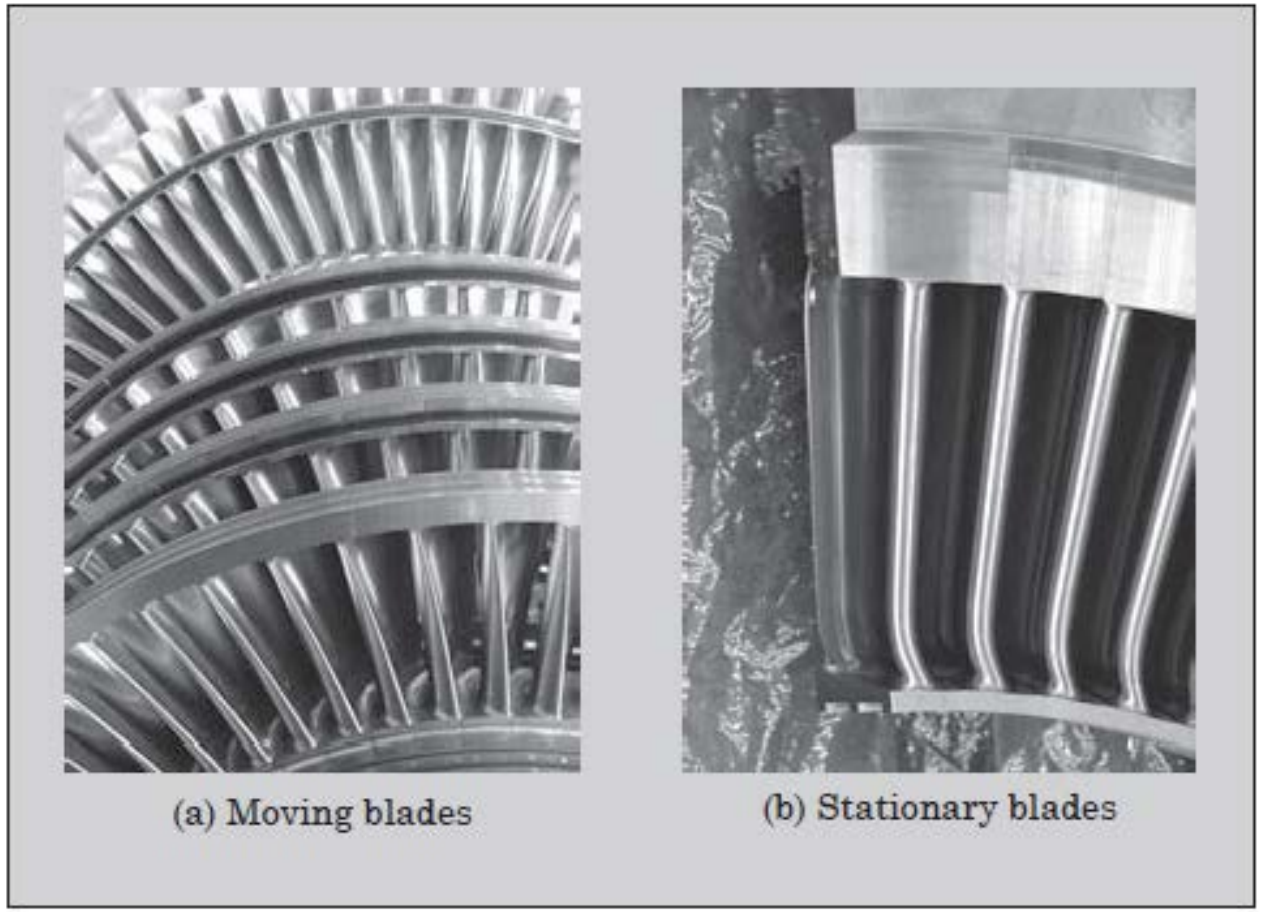

Yoshihiro Sakai , Yoshiki Oka, Hideo Kato , The Latest Geothermal Steam Turbines, Vol. 55 No. 3 **FUJI ELECTRIC REVIEW**

Erosion

Table 1 Standard materials for geothermal turbines

Part	Standard material
Blade material	13% Cr steel 16% Cr-4% Ni steel Ti-6% Al-4% V alloy
Rotor material	1% Cr-MoNiV steel 2% Cr-MoNiWV steel

Table 2 Series of new-generation low-pressure blades for geothermal steam turbines

50 Hz use (nominal annular area)	60 Hz use (nominal annular area)
348 mm blade (1.6 m^2)	290 mm blade (1.1 m^2)
487 mm blade (2.5 m^2)	406 mm blade (1.7 m^2)
555 mm blade (3.2 m^2)	462 mm blade (2.2 m^2)
612 mm blade (4.0 m^2)	510 mm blade (2.8 m^2)
697 mm blade (5.0 m^2)	581 mm blade (3.5 m^2)
798 mm blade (6.3 m^2)	665 mm blade (4.4 m^2)

Johnson W. Ndege, MAINTENANCE CHALLENGES IN THE OPERATION OF A GEOTHERMAL POWER STATION: A CASE FOR OLKARIA II PLANT – KENYA, GEOTHERMAL TRAINING PROGRAMME, Reports 2006

Yoshihiro Sakai , Yoshiki Oka, Hideo Kato , The Latest Geothermal Steam Turbines, Vol. 55 No. 3 **FUJI ELECTRIC REVIEW**

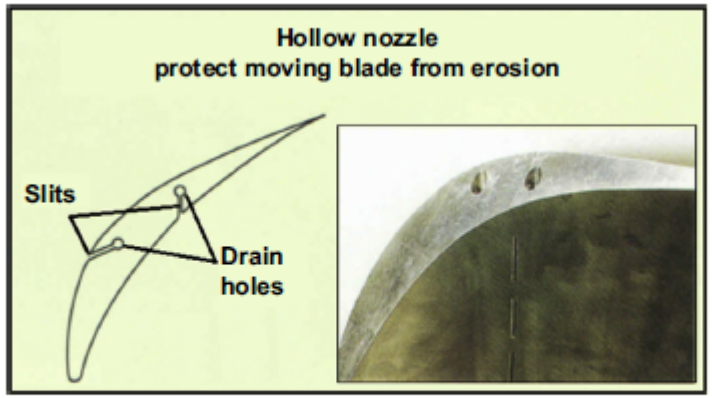

Figure 11.3 Steam turbine moisture removal – Mitsubishi.
Development of Large Capacity Single Cylinder Geothermal Turbine paper presented at the 1998 GRC Annual Meeting.

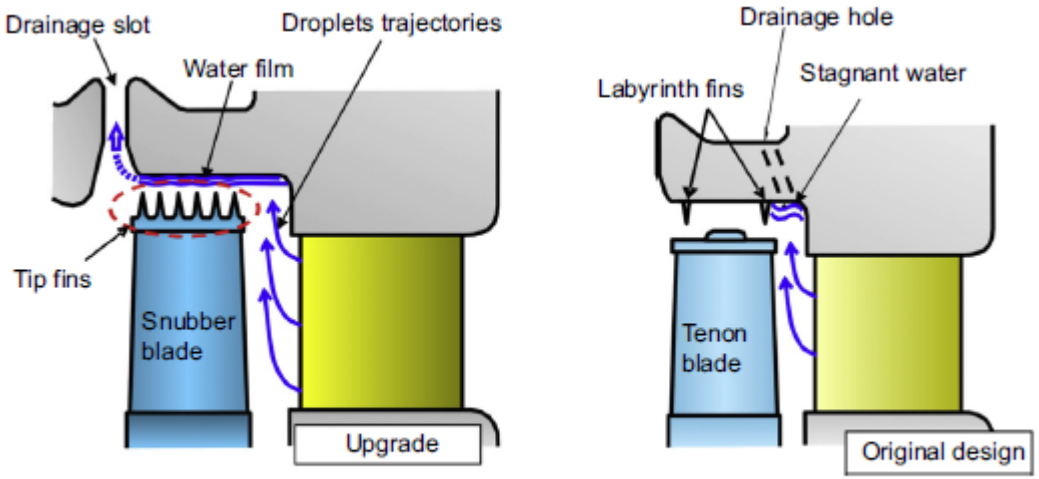

Figure 11.4 Steam turbine moisture removal – Toshiba.
Turbine Upgrade for Geysers Power Plant paper presented at the 2011 GRC Annual Meeting.

Ronald DiPippo, Geothermal Power Generation Developments and Innovation, Elsevier 2016

Fig.8 Sectional view of Wayang Windu Unit 2 geothermal steam turbine

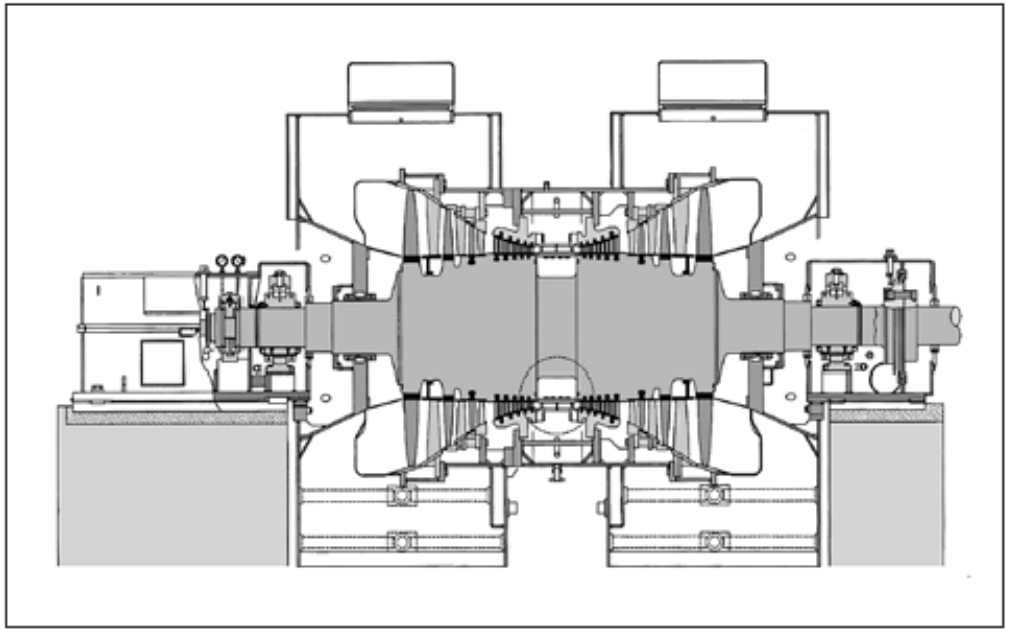

Table 3 Main specifications of Wayang Windu Unit 2 geothermal steam turbine

Turbine type	Single-casing dual-exhaust condensing
Generator output	117.0 MW
Rotating speed	3,000 r/min
Inlet steam condition	1.07 MPa, 182.8 °C (saturated)
Effective strength of last stage blades	697 mm
Nominal annular area	5.0 m^2

in order to provide enhanced corrosion resistance, the coating technology has been applied to the rotor and other parts of the turbine. The gross output of 117.0 MW is the world's largest for a single-casing type geothermal steam turbine

Yoshihiro Sakai , Yoshiki Oka, Hideo Kato , The Latest Geothermal Steam Turbines, Vol. 55 No. 3 **FUJI ELECTRIC REVIEW**

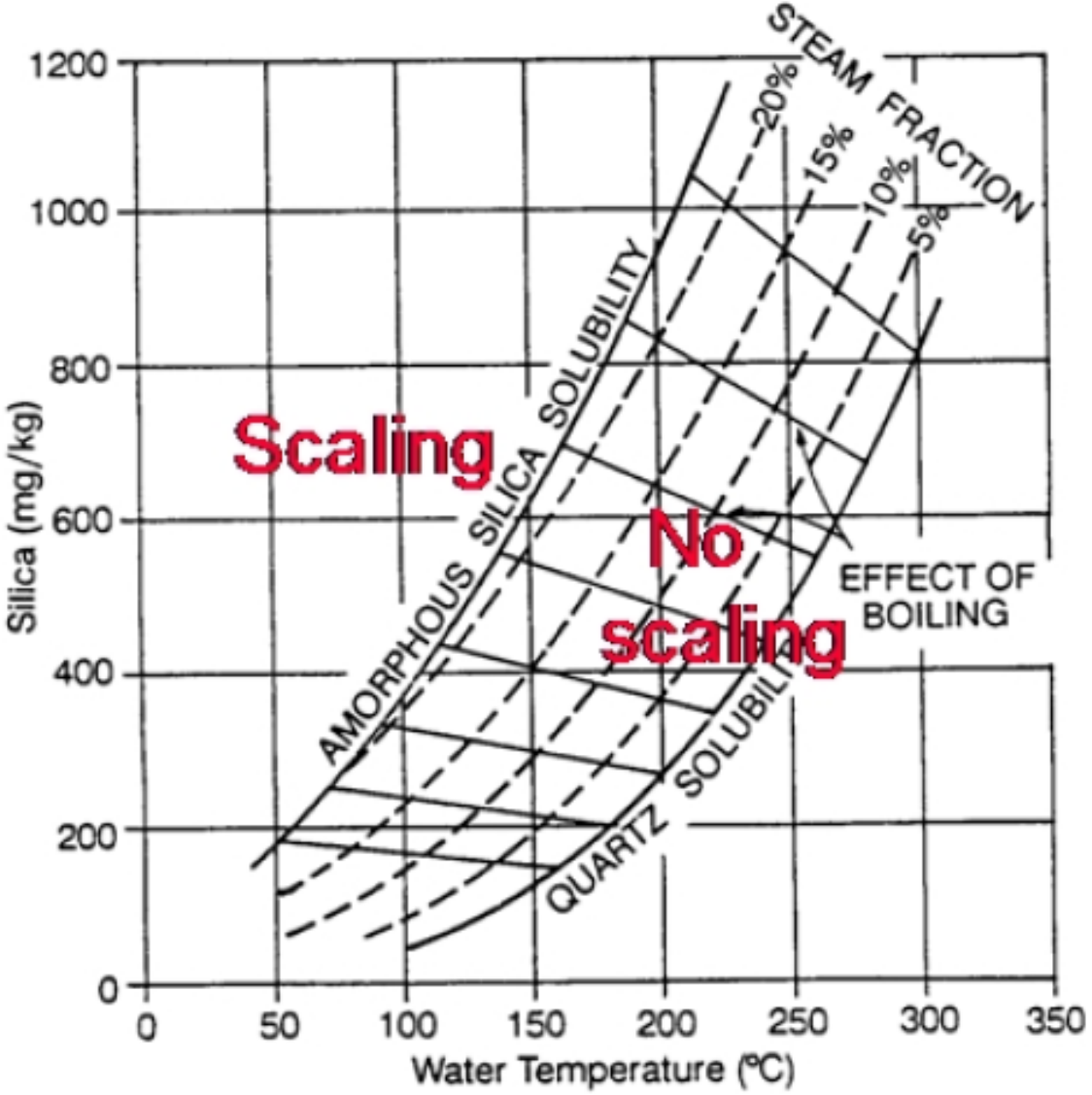

FIGURE 1: Solubility of silica in water. Scaling occurs above the amorphous silica solubility curve.

Einar Gunnlaugsson, Halldór Ármannsson, Sverrir Thorhallsson and Benedikt Steingrímsson,
PROBLEMS IN GEOTHERMAL OPERATION – SCALING AND CORROSION ,
"Short Course VI on Utilization of Low- and Medium-Enthalpy Geothermal Resources and Financial Aspects of Utilization",

Condenser

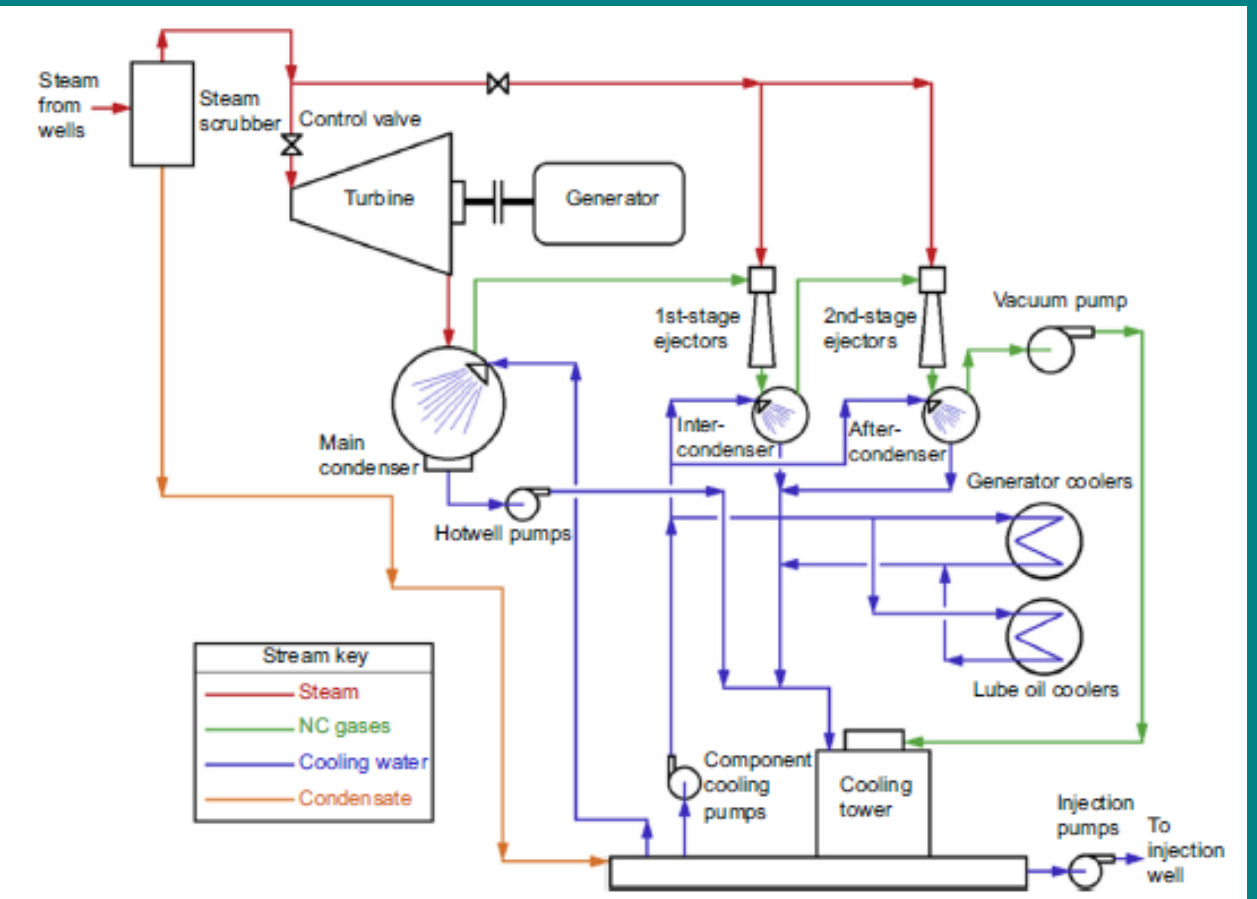

Figure 11.1 Geothermal steam power cycle – direct contact condenser.

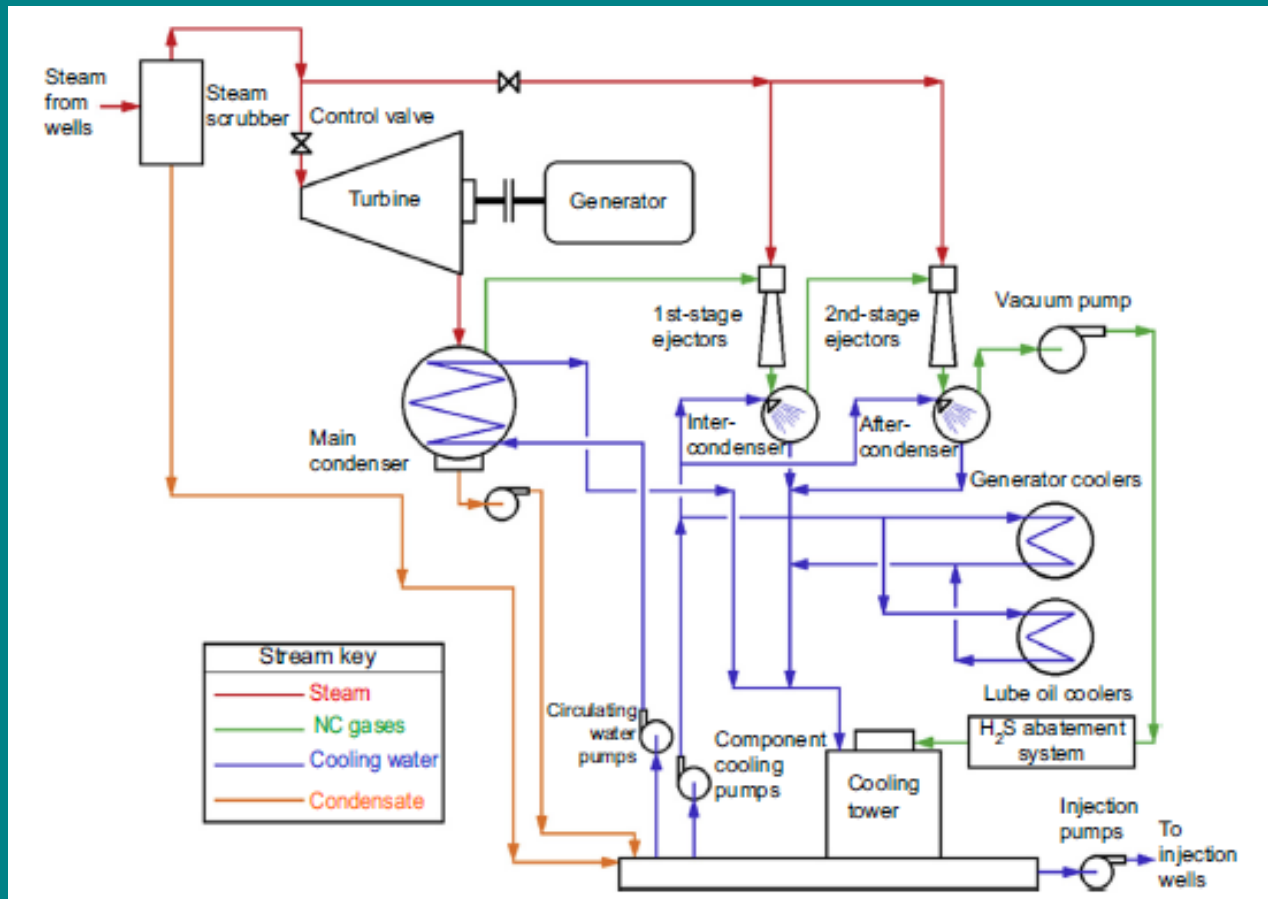

Figure 11.2 Geothermal steam power cycle – surface condenser.

Ronald DiPippo, Geothermal Power Generation Developments and Innovation, Elsevier 2016

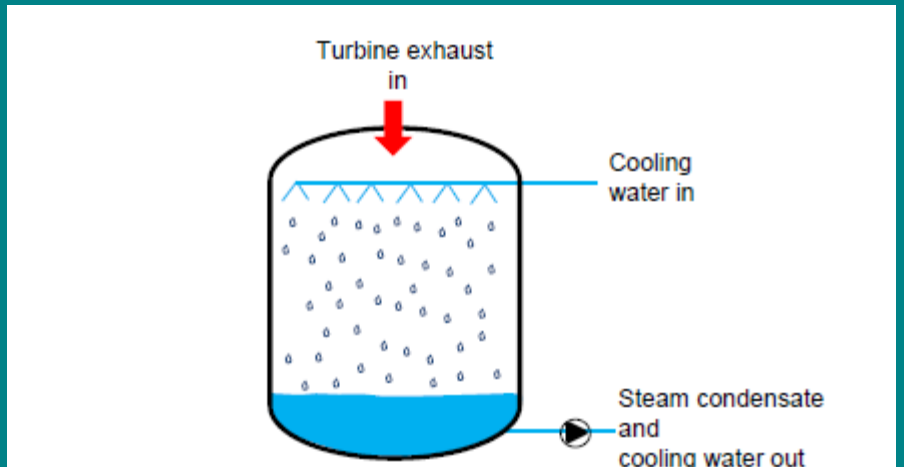

Figure 15.3 Schematic of a direct-contact steam condenser.

Ronald DiPippo, Geothermal Power Generation Developments and Innovation, Elsevier 2016

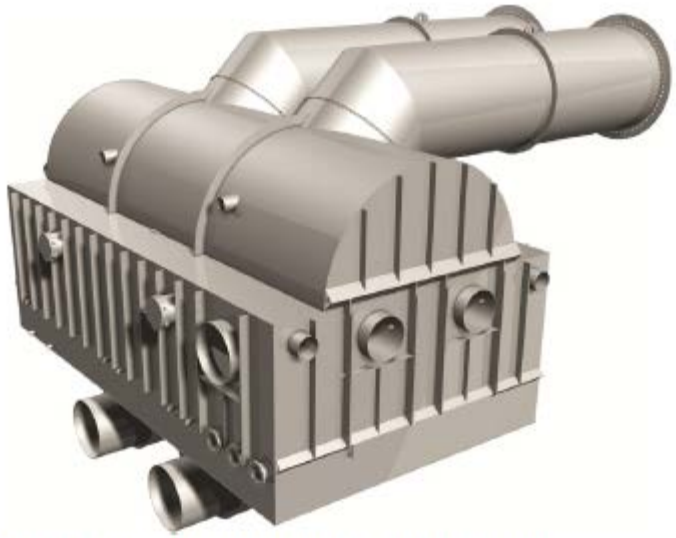

Figure 11.5 Advanced direct contact condenser – external view. ADCC Geothermal Condenser cut sheet (IN-HT2-14.pdf).

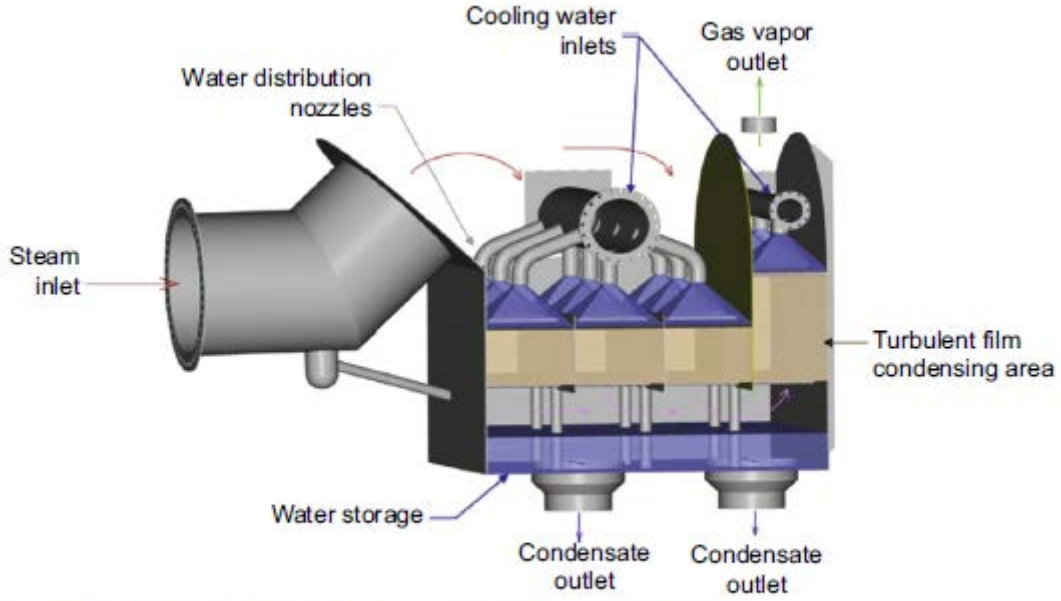

Figure 11.6 Advanced direct contact condenser – cutaway view. ADCC Geothermal Condenser cut sheet (IN-HT2-14.pdf).

Ronald DiPippo, Geothermal Power Generation Developments and Innovation, Elsevier 2016

Cooling Tower

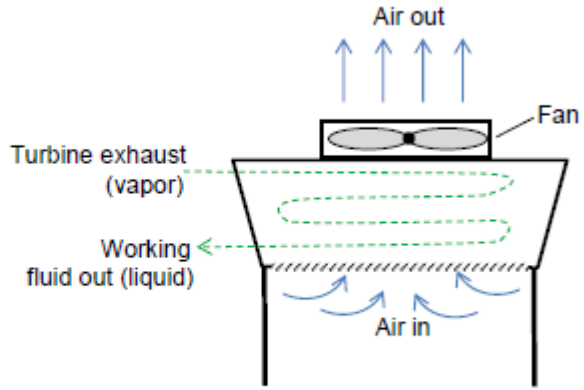

Figure 15.8 Schematic of an air-cooled condenser.

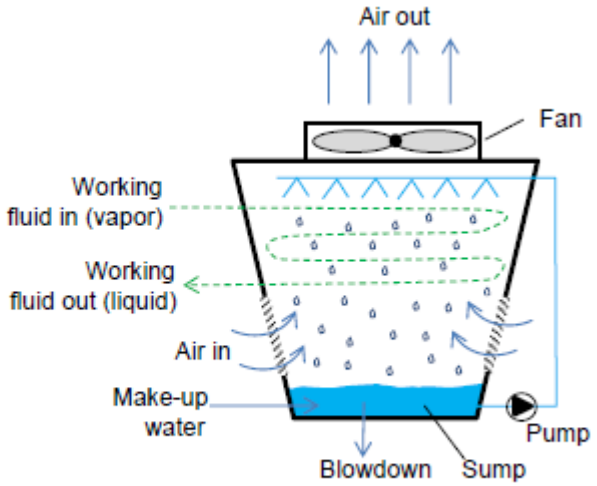

Figure 15.9 Schematic of an evaporative condenser.

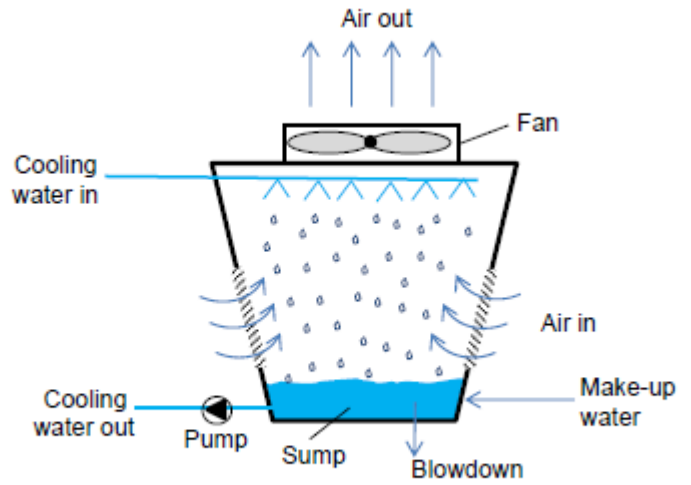

Figure 15.6 Schematic of a mechanical draft, counterflow wet cooling tower.

Ronald DiPippo, Geothermal Power Generation Developments and Innovation, Elsevier 2016

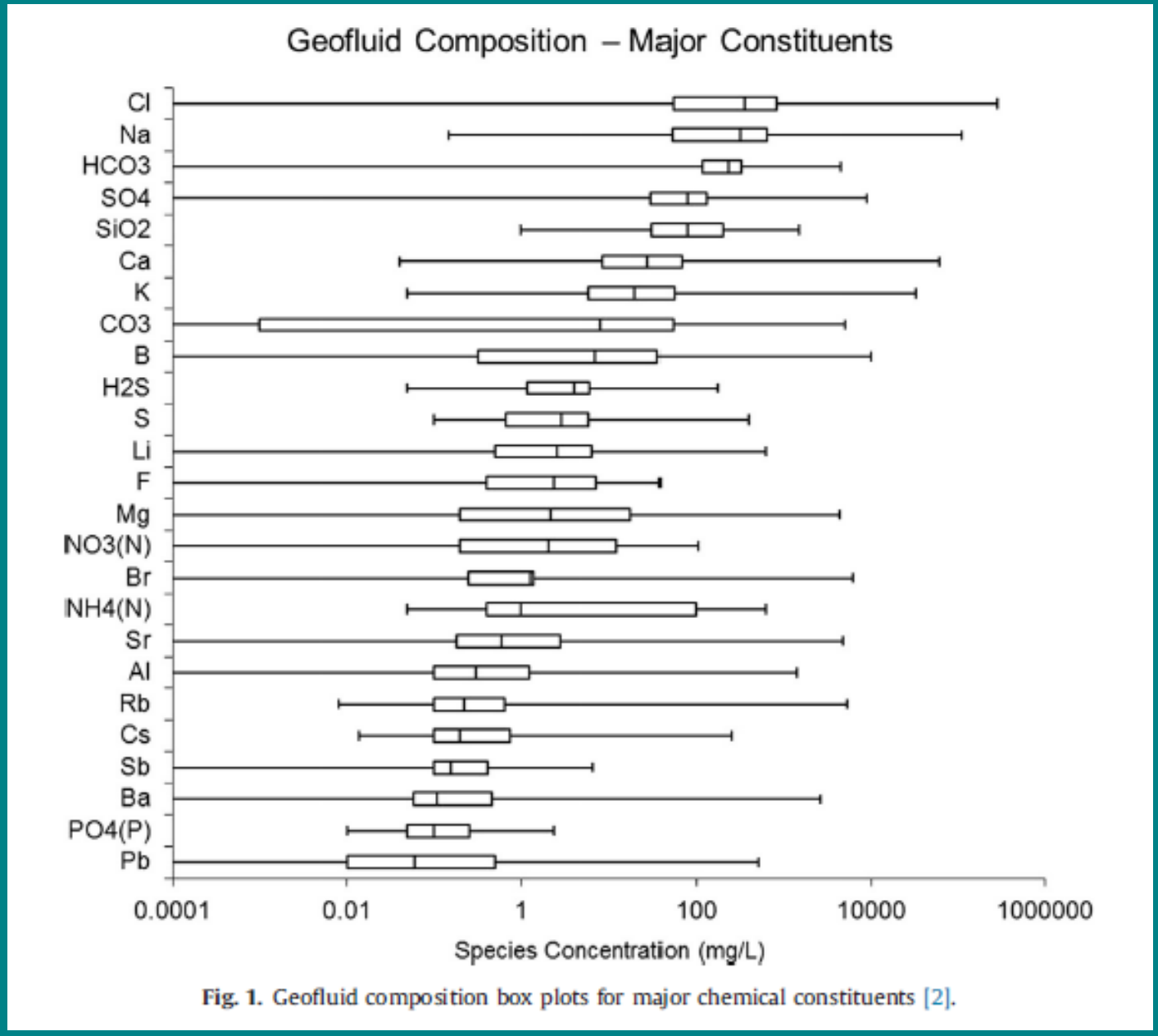

Fig. 1. Geofluid composition box plots for major chemical constituents [2].

Finster , et al. RenewableandSustainableEnergyReviews50(2015)952–966

Table 3
Summary of scale and corrosion formation mechanisms and process mitigation options for geothermal produced fluid.

Chemical species	Drivers of scale formation	Mitigation options
Silicon dioxide (silica)	↓ Temperature Near-neutral pH ↑ Dissolved silica concentration	- Modification of system operating conditions to minimize oversaturation - Modification of geofluid pH via acidification - Modification of geofluid using non-pH-adjusting compounds or reducing agents
Metal sulfide	↓ Temperature ↑ pH ↓ Oxidation state ↓ Dissolved hydrogen sulfide concentration	- Mechanical removal - Oxidation of geofluid - Acidification of geofluid
Calcium carbonate (calcite)	↑ Temperature ↑ pH ↓ Dissolved carbon dioxide concentration	- Pressurization of geofluid in the wellbore - Injection of specialized scale inhibitors - Acidification of geofluid
Corrosion	↑Temperature ↓pH ↑Salinity ↑Chloride concentration ↑Dissolved gas concentration (carbon dioxide, hydrogen sulfide, ammonia, and oxygen)	- Use of corrosion-resistant materials or coatings - Removal of corrosive species - Treatment of brines with reducing agents

Finster , et al. RenewableandSustainableEnergyReviews50(2015)952–966

Table 3. Fluid impact on the metal equipment of GeoPP

Type of impact	Damage cause	Typical trouble spot	Operation condition
General corrosion	Aggressiveness of geothermal medium: low pH, high temperature, presence CO_2, H_2S, Cl, O_2, etc.	Almost all main GeoPP's elements	Stagnant areas, small flow rates
Chloride stress cracking	Metal stress state in the presence of chlorides	Blades, wheels and turbine rotor	Phase transition area
Hydrogen sulphide stress cracking	Metal stress stete in the presence of hydrogen sulfide	Drill pipeswater	High temperature, superheated steam
Flow accelerated corrosion	Metal corrosion in combination with the hydrodynamic flow impact	Water and wet steam pipelines, turbine, separators, evaporators components, valves, etc.	High flow rate and turbulence
Droplet impingement erosion	Water droplets against metal impingement	Turbine blades	High wet steam flow rates
Cavitation erosion	Cavitation effect on metal	Pumps, valves	High aqueous medium rate, pressure fall-off
Carbonate deposits	Presence of dissolved CO_2, pH growth	Fluid transport pipes	Temperature of up to 250°C, flow turbulence
Sulphide deposits	Metal corrosion in the presence of H_2S	Pipelines, wheelspace, valves, evaporators, etc.	At a low temperature

G. V. Tomarov and A. A. Shipkov, Modern Geothermal Power: GeoPP with Geothermal Steam Turbines,
Thermal Engineering, 2017, Vol. 64, No. 3, pp. 190–200.

Fig. 2. Corrosion product from the outermost set of labyrinth packing.

Fig. 3. Corrosion product sample taken from the labyrinth packing.

(a)

(b)

Fig. 7. (a) Erosive wear of rotor blade leading edges of the last turbine stage and (b) deposits in the nozzle-blade cascade.

G. V. Tomarov and A. A. Shipkov, Modern Geothermal Power: GeoPP with Geothermal Steam Turbines, *Thermal Engineering, 2017, Vol. 64, No. 3, pp. 190–200.*

Thank You